

Biquandle Coloring Invariants of Knotoids

Neslihan Gügümcü*

Sam Nelson†

Abstract

In this paper, we consider biquandle colorings for knotoids in \mathbb{R}^2 or S^2 and we construct several coloring invariants for knotoids derived as enhancements of the biquandle counting invariant. We first enhance the biquandle counting invariant by using a matrix constructed by utilizing the orientation a knotoid diagram is endowed with. We generalize Niebrzydowski's biquandle longitude invariant for virtual long knots to obtain new invariants for knotoids. We show that biquandle invariants can detect mirror images of knotoids and show that our enhancements are proper in the sense that knotoids which are not distinguished by the counting invariant are distinguished by our enhancements.

KEYWORDS: Knotoids, biquandles, enhancements of counting invariants

2010 MSC: 57M27, 57M25

1 Introduction

Knotoids, introduced by Turaev in [17], are knotted curves immersed in surfaces with two endpoints which are not allowed to move over or under another strand, generalizing the notion of $(1, 1)$ -tangle to allow endpoints in different regions of the planar complement of the knotoid. Knotoids and their invariants are the subject of much recent study [9, 10, 11, 12, 8].

Biquandles are algebraic structures with axioms encoding the oriented Reidemeister moves; they are used to define invariants of oriented knots and links by counting colorings. Introduced in [5], they have also been the subject of much recent study [4]. In particular, biquandle-colored knots and links form a category whose invariants can be used to define invariants of knots and links known as *enhancements* of the counting invariant [4, 2, 14, 15].

Longitudes in the knot group are elements of the knot group which are homotopic to the knot itself; these have been studied in various contexts such as [13]. In [16] a type of enhancement of the biquandle counting invariant of virtual long knots was defined using a biquandle version of longitudes, known as *biquandle longitude invariants*.

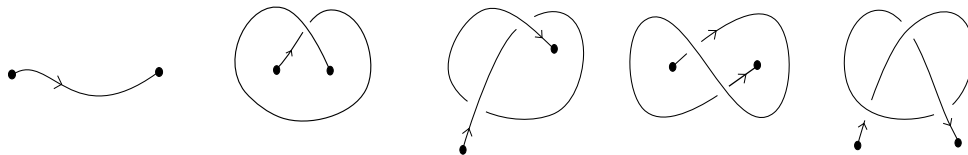
In this paper we consider biquandle colorings of knotoids and introduce several enhancements of the biquandle counting invariant. First, we introduce a matrix-valued enhancement of the counting invariant making use of the special structure of knotoids. Next, we apply the biquandle longitude enhancement idea to the case of knotoids, obtaining several enhanced invariants in the process. The paper is organized as follows. In Section 2 we recall the basics of knotoids. In Section 3 we review biquandles and the biquandle counting invariant, which can be defined for knotoids without any further modification, and we use the fact that biquandle colorings of knotoids are fixed at the endpoints to enhance the counting invariant, obtaining a matrix-valued invariant. In Section 4.2 we define several longitude enhancements for knotoids and give some examples. We show that biquandle invariants can detect mirror images of knotoids and show that our enhancements are proper in the sense that knotoids which are not distinguished by the counting invariant are distinguished by our enhancements. We conclude in Section 5 with some questions for future work.

*Email: nesli@central.ntua.gr

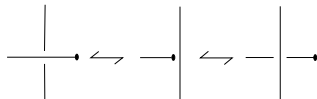
†Email: Sam.Nelson@cmc.edu. Partially supported by Simons Foundation collaboration grant 316709

2 Knotoids

Knotoid diagrams are open ended oriented knot diagrams in oriented surfaces, forming new diagrammatic theories, including an extension of the classical knot theory when the supporting surface of the knotoid is considered to be the 2-sphere S^2 [17]. A *knotoid diagram* K in a surface Σ is a generic immersion of the unit interval $[0, 1]$ into Σ with two distinct endpoints as images of 0 and 1, named as the *tail* and *head* of K , a finite number of self-crossing points that are transverse double points endowed with extra passage information of over/under, and endowed with the orientation of $[0, 1]$ from left to right (see Figure 1, for examples). A $(1, 1)$ -tangle or a long knot is defined to have its endpoints in a single region of the diagram. A knotoid diagram generalizes the notion of $(1, 1)$ - tangle or long knot by allowing its two endpoints to lie in different regions of the diagram. Below are some examples of knotoid diagrams considered in S^2 or \mathbb{R}^2 :



A *knotoid* in a surface is defined to be an equivalence class given by the isotopy relation generated by three Reidemeister moves each taking place in local disks disjoint from the endpoints of the knotoid diagram, and isotopy of the supporting surface [17]. The *trivial knotoid* is a knotoid admitting a diagram without any crossings in its equivalence class. We forbid the following two moves



displacing an endpoint by sliding it over/under a transversal strand. The ban of these moves yields a non-trivial theory of knotoids.

The theory of knotoids was introduced by Vladimir Turaev [17] in 2012 and further studied by the first author and Louis Kauffman [9] with the introduction of new invariants for knotoids. We also have a classification table of spherical knotoids up to 5 crossings given by Andrew Bartholomew [1] given by the use of a generalization of the bracket polynomial for knotoids introduced by Turaev [17]. Furthermore, geometric interpretations of knotoids (both planar and spherical) given in [9, 10] make it an eligible theory for understanding physical structures, for instance see [6, 7] for topological modeling of open linear protein chains via spherical and planar knotoids. Recently, a braided counterpart theory to the theory of planar knotoids, namely the theory of braidoids, has been introduced by the first author and Sofia Lambropoulou [12]. In [11, 12], they proved analogues of the Alexander theorem and the Markov theorem for knotoids/multi-knotoids and braidoids.

3 Biquandles and the Counting Invariant

In this section, we review biquandles and the biquandle counting invariant. There is a variety for the choice of notation in defining a biquandle, we will find the notation in [3] most suitable for the purposes of this paper.

Definition 1. Let X be a set. A *biquandle structure* on X is an assignment of two bijections $\alpha_b, \beta_b : X \rightarrow X$ to each element $b \in X$ such that the following axioms are satisfied:

- (i) For all $a \in X$, $\alpha_a(a) = \beta_a(a)$,

(ii) For all $a, b \in X$, the map $S : X \times X \rightarrow X$ defined by

$$S(a, b) = (\alpha_a(b), \beta_b(a))$$

is invertible, and

(iii) For all $a, b \in X$ we have the *exchange laws*:

$$\begin{aligned} \alpha_{\alpha_a(b)}\alpha_a &= \alpha_{\beta_b(a)}\alpha_b & \text{(iii.i)} \\ \beta_{\alpha_a(b)}\alpha_a &= \alpha_{\beta_b(a)}\beta_b & \text{(iii.ii)} \\ \beta_{\beta_a(b)}\beta_a &= \beta_{\alpha_b(a)}\beta_b & \text{(iii.iii)} \end{aligned}$$

Example 1. Examples of biquandles include

- *Constant Action Biquandles*: For any set X and bijection $\sigma : X \rightarrow X$, the assignment $\alpha_b = \beta_b = \sigma$ define a biquandle structure in which the actions α_b, β_b do not depend on b .
- *Alexander Biquandles*: For any module over the 2-variable Laurent polynomial ring $\mathbb{Z}[t^{\pm 1}, s^{\pm 1}]$, the maps

$$\alpha_b(a) = sa \quad \text{and} \quad \beta_b(a) = ta + (s - t)b$$

define a biquandle structure.

- *Quandles*: A biquandle in which α_b is the identity map for all b , is a *quandle*. Examples include groups with $\beta_b(a) = b^{-n}ab^n$ for $n \in \mathbb{Z}$ (known as *n-fold conjugation quandles*), groups with $\beta_b(a) = ab^{-1}a$ (known as *core quandles*), and vector spaces with $\beta_b(a) = a + \langle a, b \rangle b$ for a symplectic form $\langle \cdot, \cdot \rangle$ (known as *symplectic quandles*) as well as many more.

See [4] for more.

Example 2. We can represent biquandle structures on the finite set $X = \{1, 2, \dots, n\}$ by listing the maps $\beta_1, \dots, \beta_n, \alpha_1, \dots, \alpha_n$ as column vectors in an $n \times 2n$ block matrix with the first through n th columns being β_1 through β_n and the $n + 1$ st through $2n$ th columns being α_1 through α_n , as any map $\sigma : X \rightarrow X$ can be represented by the column vector

$$\begin{bmatrix} \sigma(1) \\ \sigma(2) \\ \vdots \\ \sigma(n) \end{bmatrix}.$$

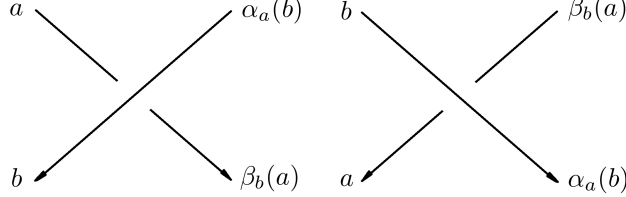
For instance, the Alexander biquandle structure on \mathbb{Z}_4 with $t = 1$ and $s = 3$ has matrix

$$\left[\begin{array}{cccc|cccc} 3 & 1 & 3 & 1 & 3 & 3 & 3 & 3 \\ 4 & 2 & 4 & 2 & 2 & 2 & 2 & 2 \\ 1 & 3 & 1 & 3 & 1 & 1 & 1 & 1 \\ 2 & 4 & 2 & 4 & 4 & 4 & 4 & 4 \end{array} \right].$$

Then for example in cycle notation we have $\beta_1 = (13)(24)$ and $\alpha_1 = (13)$ while $\beta_2 = ()$ where $()$ stands for the identity permutation, and $\alpha_2 = (13)$. The notation is chosen so that the two block matrices are the operation tables for the binary operations $\triangleright, \triangleright$ on X defined by $x \triangleright y = \beta_y(x)$ and $x \triangleright y = \alpha_y(x)$.

Definition 2. Let K be a knotoid in S^2 or \mathbb{R}^2 represented by a diagram D and X a biquandle. A *semiarc* of D is defined to be a piece of strand of D that connects either two adjacent crossings or an endpoint to a crossing. A *biquandle coloring* of D by X is an assignment of an element of X to each semiarc in D such that at every crossing the local coloring is as illustrated in the figure below. Here we label (or color) the four semiarcs neighboring a positive and a negative crossing, respectively and all directed downwards. The

left-hand side colors $a, b \in X$ are considered to be the inputs for the corresponding biquandle bijections on X , β_b and α_a , respectively. The upper right semiarc is colored with the output color $\alpha_a(b)$ and the lower right semiarc is colored $\beta_b(a)$, if the crossing is positive. If the crossing is negative then the upper right semiarc is colored $\beta_b(a)$ and the lower right semiarc is colored $\alpha_a(b)$.



Similarly to the case of (classical/virtual) knots, the biquandle axioms are set so that for any diagram with a biquandle coloring before a Reidemeister move, there is a unique coloring of the diagram after the move which agrees with the previous coloring outside the neighborhood of the move. It follows that the number of such colorings is an invariant of knotoids. We will denote the set of biquandle colorings of a knotoid diagram D by a biquandle X as $\mathcal{C}(D, X)$.

Definition 3. Let X be a finite biquandle and D a knotoid diagram representing a knotoid K . Then the *biquandle counting invariant* of K is the cardinality $\Phi_X^{\mathbb{Z}}(K) = |\mathcal{C}(D, X)|$ of the set of colorings of D by X .

Example 3. We can compute $\Phi_X^{\mathbb{Z}}(K)$ from any diagram of K by listing all possible assignments of elements of X to the semiarcs in K and noticing which ones satisfy the crossing relations pictured in Definition 2. For example, the knotoid diagram below has five semiarcs and four crossing equations; arbitrarily selecting a and b in X determines $c = \alpha_a(b)$, $d = \beta_b(a)$ and $e = \beta_c(b) = \beta_{\alpha_a(b)}(b)$, so the coloring is valid provided we have $d = \beta_b(a) = \alpha_b(c) = \alpha_b(\alpha_a(b))$. Then for instance if $X = \{1, 2, 3, 4, 5\}$ is equipped with the biquandle structure determined with the listed matrix below, we can check the required equation for each assignment of elements of X to a, b .

$$X = \left[\begin{array}{ccccc|ccccc} 3 & 1 & 3 & 1 & 1 & 3 & 3 & 3 & 3 & 3 \\ 5 & 4 & 5 & 2 & 5 & 5 & 4 & 5 & 4 & 4 \\ 1 & 3 & 1 & 3 & 3 & 1 & 1 & 1 & 1 & 1 \\ 2 & 2 & 2 & 5 & 4 & 2 & 5 & 2 & 5 & 5 \\ 4 & 5 & 4 & 4 & 2 & 4 & 2 & 4 & 2 & 2 \end{array} \right]$$

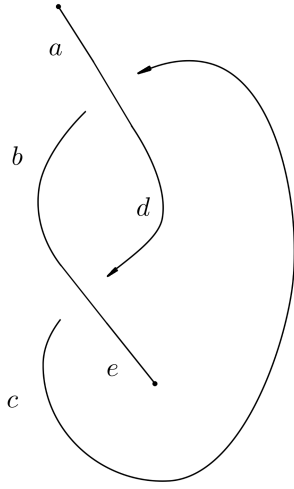
a	b	$\beta_b(a) = \alpha_b(\alpha_a(b))?$	a	b	$\beta_b(a) = \alpha_b(\alpha_a(b))?$
1	1	—	3	4	—
1	2	—	3	5	—
1	3	✓	4	1	—
1	4	—	4	2	—
1	5	—	4	3	—
2	1	—	4	4	—
2	2	—	4	5	✓
2	3	—	5	1	—
2	4	✓	5	2	✓
2	5	—	5	3	—
3	1	✓	5	4	—
3	2	—	5	5	—
3	3	—			

Hence in this example we see that $\Phi_X^{\mathbb{Z}}(K) = 5$.

Example 4. Let X be the biquandle with matrix

$$\left[\begin{array}{ccc|ccc} 2 & 1 & 3 & 2 & 2 & 2 \\ 1 & 3 & 2 & 3 & 3 & 3 \\ 3 & 2 & 1 & 1 & 1 & 1 \end{array} \right].$$

As can be verified by the table below, the knotoid in Example 3 has three colorings by X . We see that for coloring the mirror image knotoid obtained by over-under switching all of the crossings of D , the equation $d = \alpha_b(a) = \beta_b(c) = \beta_b(\beta_a(b))$ should be satisfied. It is verified in the same table that the mirror image knotoid has no colorings by X ; hence the biquandle counting invariant shows that this knotoid is not equivalent to its mirror image and that biquandle counting invariants can detect this type of mirror image in knotoids.



a	b	$\alpha_b(a) = \beta_b(\beta_a(b))?$	$\beta_b(a) = \alpha_b(\alpha_a(b))?$
1	1	$2 \neq 1$	$2 \neq 3$
1	2	$2 \neq 1$	$1 = 1 \checkmark$
1	3	$2 \neq 1$	$3 \neq 2$
2	1	$3 \neq 2$	$1 \neq 3$
2	2	$3 \neq 2$	$3 \neq 1$
2	3	$3 \neq 2$	$2 = 2 \checkmark$
3	1	$1 \neq 3$	$3 = 3 \checkmark$
3	2	$1 \neq 3$	$2 \neq 1$
3	3	$1 \neq 3$	$1 \neq 2$

Example 5. For Alexander biquandles of the form $X = \mathbb{Z}_n$ with s, t coprime to n , we can find the set of colorings via linear algebra since the coloring equations

$$\alpha_a(b) = sb \quad \text{and} \quad \beta_b(a) = ta + (s - t)b$$

are linear. The knotoid K in Example 3 has system of coloring equations

$$\begin{aligned} \beta_b(a) &= d \\ \alpha_a(b) &= c \\ \beta_c(b) &= e \\ \alpha_b(c) &= d \end{aligned}$$

which for an Alexander biquandle becomes

$$\begin{aligned} ta + (s - t)b &= d \\ sb &= c \\ tb + (s - t)c &= e \\ sc &= d. \end{aligned}$$

Then for example to find colorings of K by the Alexander biquandle $X = \mathbb{Z}_5$ with $t = 2$ and $s = 3$, we can find the kernel of the homogeneous system's coefficient matrix over \mathbb{Z}_5 :

$$\begin{bmatrix} 2 & 1 & 0 & 4 & 0 \\ 0 & 3 & 4 & 0 & 0 \\ 0 & 2 & 1 & 0 & 4 \\ 0 & 0 & 3 & 4 & 0 \end{bmatrix} \leftrightarrow \begin{bmatrix} 1 & 0 & 0 & 4 & 0 \\ 0 & 1 & 0 & 1 & 0 \\ 0 & 0 & 1 & 3 & 0 \\ 0 & 0 & 0 & 0 & 1 \end{bmatrix}$$

so in this case the kernel is one-dimensional spanned by $(1, 4, 2, 1, 0)$ and there are $|X| = 5$ colorings.

4 Enhancements of the Counting Invariant

4.1 Biquandle counting matrix

Unlike the case of classical and virtual knots, a biquandle-colored knotoid has a well-defined initial color and terminal color assigned to the semiarcs adjacent to endpoints. We make use of this feature to enhance the counting invariant as follows.

Definition 4. Let $X = \{x_1, \dots, x_n\}$ be a finite biquandle and let $\mathcal{C}_{jk}(K)$ be the set of X -colorings of K in which the initial semiarc is colored x_j and the final semiarc is colored x_k . Then the *biquandle counting matrix* of K with respect to X is the matrix $\Phi_X^{M_n}(K)$ whose entry in row j column k is $|\mathcal{C}_{jk}(K)|$.

Theorem 1. For any finite biquandle X , $\Phi_X^{M_n}(K)$ is an invariant of knotoids.

Proof. This follows immediately from the facts Reidemeister moves take place away from the endpoints so that the biquandle colorings of the initial and the terminal semiarcs and also that biquandle coloring numbers are unchanged by Reidemeister moves. \square

Corollary 2. For any knotoid K and finite biquandle X , we have

$$\Phi_X^{\mathbb{Z}}(K) = \sum_{1 \leq j, k \leq n} (\Phi_X^{M_n}(K))_{j,k}.$$

That is, the biquandle counting invariant is the sum of the entries of the biquandle counting matrix.

Example 6. We computed the biquandle coloring matrix for each of the knotoids in the table at [1] with respect to the biquandle in Example 4. The results are listed in the table.

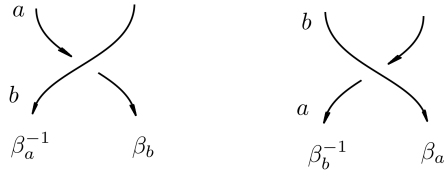
$\Phi_X^{M_n}(K)$	K
$\begin{bmatrix} 0 & 0 & 0 \\ 0 & 0 & 0 \\ 0 & 0 & 0 \end{bmatrix}$	2.1, 4.4, 4.5, 5.1, 5.2, 5.3, 5.4, 5.10, 5.11, 5.12, 5.13, 5.14, 5.15, 5.16, 5.18, 5.21, 5.23
$\begin{bmatrix} 0 & 0 & 1 \\ 1 & 0 & 0 \\ 0 & 1 & 0 \end{bmatrix}$	3.1, 4.3, 4.6, 4.7, 5.7, 5.27, 5.29
$\begin{bmatrix} 0 & 1 & 0 \\ 0 & 0 & 1 \\ 1 & 0 & 0 \end{bmatrix}$	4.1, 4.2, 4.8, 5.8, 5.19, 5.20, 5.26, 5.28
$\begin{bmatrix} 1 & 0 & 0 \\ 0 & 1 & 0 \\ 0 & 0 & 1 \end{bmatrix}$	4.9, 5.5, 5.6, 5.9, 5.22, 5.24, 5.25
$\begin{bmatrix} 3 & 0 & 0 \\ 0 & 3 & 0 \\ 0 & 0 & 3 \end{bmatrix}$	5.17
$\begin{bmatrix} 0 & 3 & 0 \\ 0 & 0 & 3 \\ 3 & 0 & 0 \end{bmatrix}$	5.30

In this example there are three counting invariant values, namely $\Phi_X^{\mathbb{Z}}(K) = 0, 3$ and 9 , while we have six counting matrix values.

4.2 Longitude enhancements

In this section, we recall the biquandle longitude invariant and consider its application to the case of knotoids. We begin with a definition adapted from [16].

Definition 5. Let X be a finite biquandle and D_f a knotoid diagram with a coloring f by X . Traveling along the knotoid in the direction of the orientation, we encounter each crossing point twice. We will assign a bijection $\beta_L^{\pm 1} : X \rightarrow X$ to each of the two passes through each crossing, depending on the crossing sign, the type of the pass (over or under) and biquandle coloring as shown:



We can summarize the rules for defining this bijection as follows: When traveling through a crossing, the assigned bijection is β_L^{jk} where j is the crossing sign, k is 1 if we are going under and -1 if we are going over, and L is the biquandle color of the strand we see if we look to the right as we pass through the crossing.

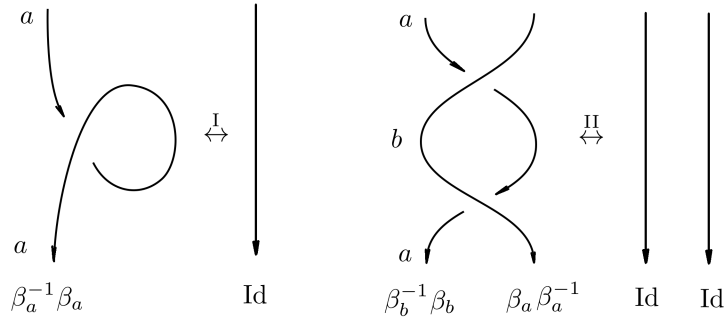
Then the *biquandle longitude weight* of the X -colored diagram D , denoted by $BLW(D_f)$, is the composition of the crossing bijections in the order in which they are encountered when traveling along the knotoid.

Remark 1. Our convention is different from that of [16], where the author chooses the color of the strand on the left. Our choice is motivated by our choice of biquandle notation, which also differs from the convention of [16].

As in [16], we have the following theorem.

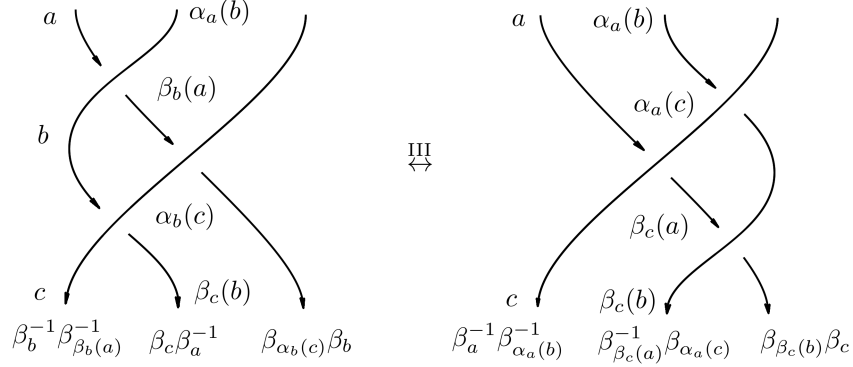
Theorem 3. $BLW(D_f)$ is not changed by biquandle-colored Reidemeister moves.

Proof. It is sufficient to check on a generating set of biquandle-colored oriented Reidemeister moves; one such set includes all four oriented moves of type I and of type II together with the Reidemeister III move with all positive crossings. In the cases of moves of type I and II, our choice of coloring rules yields an identity map on each strand.



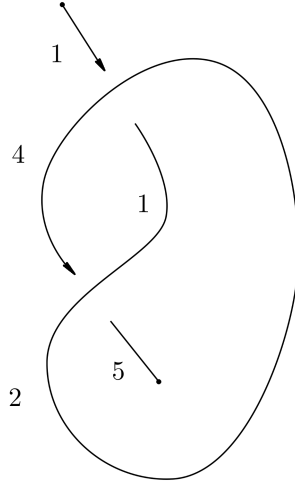
We depict one case of type I and one of type II; the others are similar. In the case of type III, the maps

induced on each of the three strands are equivalent by biquandle exchange law (iii.iii).



□

Example 7. Let us consider the X -coloring D_f of the knotoid diagram from Example 5 depicted below.



The matrix of X is given by

$$\left[\begin{array}{ccccc|ccccc} 3 & 4 & 5 & 1 & 2 & 3 & 3 & 3 & 3 & 3 \\ 5 & 1 & 2 & 3 & 4 & 1 & 1 & 1 & 1 & 1 \\ 2 & 3 & 4 & 5 & 1 & 4 & 4 & 4 & 4 & 4 \\ 4 & 5 & 1 & 2 & 3 & 2 & 2 & 2 & 2 & 2 \\ 1 & 2 & 3 & 4 & 5 & 5 & 5 & 5 & 5 & 5 \end{array} \right]$$

where our columns are numbered 1 though 5 in each block, with 5 representing the class of $0 \in \mathbb{Z}_5$ so our column labels can start with 1. We then have $\beta_1 = (1325)$, $\beta_2 = (1452)$, $\beta_3 = (1534)$, $\beta_4 = (2354)$ and $\beta_5 = (1243)$. Let us find the biquandle longitude weight for this coloring.

Traveling along the knotoid and looking to the right, we first go under a negative crossing with a strand labeled 4, then over a negative crossing with a strand labeled 4, then over a negative crossing with a strand labeled 1, then finally under a negative crossing with a strand labeled 2, so we have (composing right to left)

$$\begin{aligned} BLW(D_f) &= \beta_2^{(1)(-1)} \beta_1^{(-1)(-1)} \beta_4^{(-1)(-1)} \beta_4^{(1)(-1)} \\ &= \beta_2^{-1} \beta_1 \beta_4 \beta_4^{-1} \\ &= \beta_2 \beta_1^{-1} \\ &= (1452)(1523) = (12345) \end{aligned}$$

and this coloring has biquandle longitude weight (12345).

Definition 6. Let X be a biquandle and K a knotoid with diagram D . The *biquandle longitude multiset* invariant of K is the multiset of biquandle longitude weights over the set of biquandle colorings of K . That is,

$$\Phi_X^{M,L}(K) = \{BLW(D_f) \mid f \in \text{Hom}(\mathcal{B}(K), X)\}.$$

For ease of comparison, we can extract polynomial invariants of knotoids from $\Phi_X^{M,L}(K)$ by replacing each weight with some integer-valued invariant of bijections. For instance, we can define the *biquandle longitude exponent polynomial* $\Phi_X^{BLE}(K)$ of K by replacing each biquandle longitude weight $BLW(D_f)$ with its exponent $\exp(BLW(D_f))$, i.e. the minimal positive integer k such that $BLW(D_f)^k = \text{Id}$, and converting the resulting multiset to polynomial form by summing the power u^k of a formal variable u for each element k in the multiset. This polynomial notation has the advantage that evaluation at $u = 1$ yields the biquandle counting invariant $\Phi_X^{\mathbb{Z}}(K)$.

Example 8. The knotoid K in Example 7 has biquandle longitude multiset

$$\Phi_X^{M,L}(K) = \{(12345), (13524), (14253), (15432), ()\}$$

which yields exponent polynomial

$$\Phi_X^{\exp,L}(K) = u + 4u^5.$$

Example 9. We computed the biquandle longitude exponent polynomial for the knotoids in the table at [1] with the biquandle X given by the matrix

$$\left[\begin{array}{cccc|cccc} 1 & 2 & 1 & 4 & 1 & 1 & 1 & 1 \\ 2 & 4 & 4 & 1 & 4 & 4 & 4 & 4 \\ 3 & 3 & 3 & 3 & 3 & 3 & 3 & 3 \\ 4 & 1 & 2 & 2 & 2 & 2 & 2 & 2 \end{array} \right]$$

using our `python` code. The results are collected in the table.

$\Phi_X^{\exp,L}(K)$	K
$2u + 2u^3$	2.1, 3.1, 4.1, 4.2, 4.3, 4.5, 4.9, 5.3, 5.4, 5.7, 5.8, 5.10, 5.12 5.14, 5.16, 5.19, 5.20, 5.22, 5.23, 5.26, 5.27, 5.28, 5.29
$4u$	4.4, 4.8, 5.5, 5.6, 5.9, 5.11, 5.13, 5.15, 5.18, 5.21, 5.30
$4u + 6u^3$	4.6, 5.1, 5.2, 5.24, 5.25
$10u$	4.7, 5.17.

In particular, the two counting invariant values $\Phi_X^{\mathbb{Z}}(K) = 4, 10$ are refined into four exponent polynomial values, distinguishing more knotoids than the unenhanced counting invariant.

The longitude weight of a biquandle-colored knotoid is a bijection from the biquandle to itself, since it is composition of bijections $\beta_L^{\pm 1}$. In the case of biquandles for which we have explicit formulas for $\beta_L^{\pm 1}$, we can obtain explicit formulas for the biquandle longitudes as well. This can give us a stronger enhancement than the exponent polynomial since different longitude weights may have the same exponent, while still being easier to compare invariant values visually.

Example 10. In Example 5, the biquandle X has Alexander biquandle structure on \mathbb{Z}_5 with

$$\beta_b(x) = 2x + b \quad \text{and} \quad \beta_b^{-1}(x) = 3x + 2b.$$

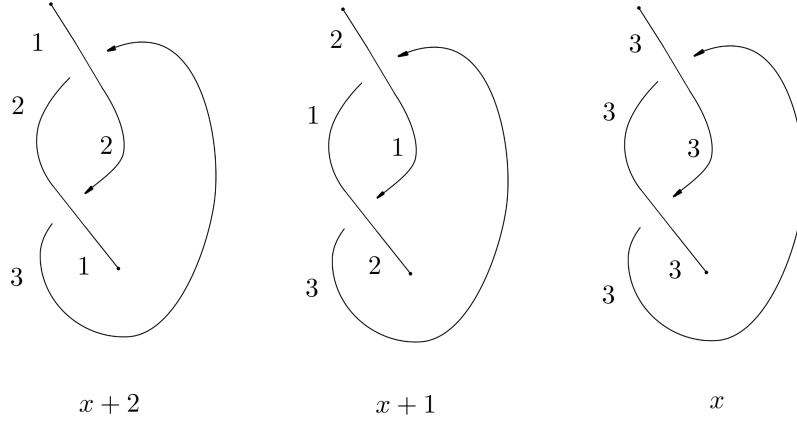
Then the longitude for the pictured coloring is the map

$$\begin{aligned} BLW(D_f)(x) &= \beta_2^{-1}(\beta_1^{-1}(x)) \\ &= \beta_2^{-1}(3x + 2(1)) \\ &= 2(3x + 1) + 2 \\ &= x + 4. \end{aligned}$$

This observation inspires the following definition.

Definition 7. Let X be an Alexander biquandle and K a knotoid. Then the *Alexander Longitude Enhancement*, denoted $\Phi_X^{M,AL}(K)$ is the multiset of biquandle longitude weights written explicitly as functions on X .

Example 11. Let $X = \mathbb{Z}_3 = \{1, 2, 3\}$ with $t = 1$ and $s = 2$. The knotoid 2.1 below has the pictured Alexander biquandle colorings by X yielding the listed longitudes.



Then comparing with the trivial knotoid, the counting invariant values are both $\Phi_X^{\mathbb{Z}}(K) = 3$ while the Alexander longitude enhancement values distinguish the knotoids, with

$$\Phi_X^{M,AL}(2.1) = \{x, x+1, x+2\} \neq \{x, x, x\} = \Phi_X^{M,AL}(\text{Trivial knotoid}).$$

We note that one can also use the α^{-1} maps in place of the β maps to obtain a generally distinct longitude weight, which we will denote by $BLW_{\alpha}(D_f)$ (and when doing so, denote $BLW(D_f) = BLW_{\beta}(D_f)$). If X is a quandle, for instance, then the α_x maps are all the identity and all of the longitude information lies in the β_x maps. For non-quandle biquandles, the information is distributed in the two maps. We can thus define a two-variable polynomial invariant of knotoids using the two weights:

Definition 8. Let X be a biquandle and K a knotoid. Then the *biquandle longitude pair multiset* is

$$\Phi_X^{M,BLW^2}(K) = \{(BLW_{\beta}(D_f), BLW_{\alpha}(D_f)) \mid D_f \in \mathcal{C}(D, X)\}$$

and the *biquandle longitude exponent pair polynomial* is

$$\Phi_X^{BLE^2}(K) = \sum_{D_f \in \mathcal{C}(D, X)} u^{\exp(BLW_{\beta}(D_f))} v^{\exp(BLW_{\alpha}(D_f))}$$

Example 12. Let X be the biquandle with matrix

$$X = \left[\begin{array}{cccc|cccc} 2 & 2 & 2 & 2 & 2 & 3 & 1 & 4 \\ 1 & 1 & 1 & 1 & 4 & 1 & 3 & 2 \\ 4 & 4 & 4 & 4 & 3 & 2 & 4 & 1 \\ 3 & 3 & 3 & 3 & 1 & 4 & 2 & 3 \end{array} \right].$$

Using our `python` code, we computed $\Phi_X^{BLE}(K)$ and $\Phi_X^{BLE^2}(K)$ for the knotoids in the table at [1].

$\Phi_X^{BLE}(K)$	K
0	4.1, 4.24.6, 4.7, 5.3, 5.4, 5.7, 5.8, 5.13, 5.14, 5.16, 5.20, 5.21
$4u$	2.1, 3.1, 4.3, 4.4, 4.5, 4.8, 4.9, 5.5, 5.6, 5.9, 5.10, 5.11, 5.12, 5.15, 5.18, 5.19, 5.26, 5.27, 5.28, 5.29, 5.30
$16u$	5.1, 5.2, 5.17, 5.22, 5.23, 5.24, 5.25.

While $\Phi_X^{BLE}(K)$ does not distinguish any knotoids on the table which are not already distinguished by the counting invariant, $\Phi_X^{BLE}(K)$ does:

$\Phi_X^{BLE^2}(K)$	K
0	4.1, 4.24.6, 4.7, 5.3, 5.4, 5.7, 5.8, 5.13, 5.14, 5.16, 5.20, 5.21
$4uv$	3.1, 4.3, 4.4, 4.5, 4.9, 5.5, 5.6, 5.9, 5.10, 5.11, 5.12, 5.15, 5.26, 5.27, 5.28, 5.29, 5.30
$4uv^2$	2.1, 4.8, 5.18, 5.19
$16uv$	5.17, 5.24, 5.25
$16uv^2$	5.1, 5.22
$12uv^2 + 4uv$	5.22, 5.23.

Finally, we can use biquandle longitude weights to further enhance the matrix version of the counting invariant, making use of both the longitude information and the initial and terminal color information, analogously to the invariants of long virtual knots described in [16].

Definition 9. Let X be a biquandle and K a knotoid with diagram D . The *biquandle longitude exponent matrix* invariant of K is the matrix $\Phi_X^{M_n, BWE}(K)$ whose entry in row j column k is $\sum_{D_f \in C_{jk}(K)} u^{BWE(D_f)}$ and the *biquandle longitude exponent pair matrix* invariant of K is the matrix $\Phi_X^{M_n, BWE^2}(K)$ whose entry in row j column k is $\sum_{D_f \in C_{jk}(K)} u^{BWE_\beta(D_f)} v^{BWE_\alpha(D_f)}$.

Example 13. Let X be the biquandle with matrix

$$X = \left[\begin{array}{cccc|cccc} 3 & 1 & 2 & 4 & 3 & 3 & 3 & 3 \\ 4 & 2 & 1 & 3 & 2 & 2 & 2 & 2 \\ 1 & 3 & 4 & 2 & 4 & 4 & 4 & 4 \\ 2 & 4 & 3 & 1 & 1 & 1 & 1 & 1 \end{array} \right].$$

Using our `python` code, we computed $\Phi_X^{M_n, BLE^2}(K)$ and for the knotoids in the table at [1]. The results are collected in the table.

$\Phi_X^{M_n, BLE^2}(K)$	K
$\begin{bmatrix} u^2v & 0 & 0 & 0 \\ 0 & uv & 0 & 0 \\ 0 & 0 & u^2v & 0 \\ 0 & 0 & 0 & u^2v \end{bmatrix}$	2.1, 3.1, 4.8, 5.18, 5.26, 5.27
$\begin{bmatrix} 0 & 0 & 0 & 0 \\ 0 & 3u^2v + uv & 0 & 0 \\ 0 & 0 & 0 & 0 \\ 0 & 0 & 0 & 0 \end{bmatrix}$	4.1, 4.2, 4.6, 4.7, 5.3, 5.4, 5.7, 5.8, 5.13, 5.14, 5.16, 5.20, 5.21
$\begin{bmatrix} uv & 0 & 0 & 0 \\ 0 & uv & 0 & 0 \\ 0 & 0 & uv & 0 \\ 0 & 0 & 0 & uv \end{bmatrix}$	4.3, 4.4, 4.5, 4.9, 5.5, 5.6, 5.9, 5.10, 5.11, 5.12, 5.15, 5.18, 5.19, 5.28, 5.29, 5.30

$\Phi_X^{M_n, BLE^2}(K)$	K
$\begin{bmatrix} 4uv & 0 & 0 & 0 \\ 0 & 4uv & 0 & 0 \\ 0 & 0 & 4uv & 0 \\ 0 & 0 & 0 & 4uv \end{bmatrix}$	5.17
$\begin{bmatrix} 4u^2v & 0 & 0 & 0 \\ 0 & 4uv & 0 & 0 \\ 0 & 0 & 4u^2v & 0 \\ 0 & 0 & 0 & 4u^2v \end{bmatrix}$	5.1, 5.2, 5.17, 5.22, 5.23, 5.24, 5.25.

Comparing the enhancements, we see that

- The unenhanced counting invariant divides the knotoids into two classes (those with four colorings and those with sixteen),
- The biquandle counting matrix refines the counting invariant into three classes with invariant values

$$\begin{bmatrix} 1 & 0 & 0 & 0 \\ 0 & 1 & 0 & 0 \\ 0 & 0 & 1 & 0 \\ 0 & 0 & 0 & 1 \end{bmatrix}, \begin{bmatrix} 0 & 0 & 0 & 0 \\ 0 & 4 & 0 & 0 \\ 0 & 0 & 0 & 0 \\ 0 & 0 & 0 & 0 \end{bmatrix} \text{ and } \begin{bmatrix} 4 & 0 & 0 & 0 \\ 0 & 4 & 0 & 0 \\ 0 & 0 & 4 & 0 \\ 0 & 0 & 0 & 4 \end{bmatrix},$$

- The biquandle longitude exponent pair polynomial enhancement refines the counting invariant into four classes with values $uv + 3u^2v$, $4uv$, $16uv$ and $4uv + 12u^2v$, and
- The biquandle longitude exponent pair matrix enhancement refines the counting invariant into five classes as shown in the table.

5 Questions

We end with some questions for future research.

A biquandle longitude weight for an X -colored knotoid is a kind of noncommutative Boltzmann weight with values in the group of permutations of elements of the coloring biquandle X . Does a non-commutative analogue of biquandle homology lurk in the shadows here?

What other enhancements can be defined for the biquandle counting invariant for knotoids? How do these invariants behave under the connected sum operation on knotoids (that is joining knotoids head-to-tail)?

Acknowledgements

The first author thanks to Simons Foundation for supporting her to visit to the second author at the Claremont McKenna College, and to the Department of Mathematics at the Claremont McKenna College for the warm hospitality during her stay there.

References

- [1] A. Bartholomew. Andrew Bartholomew's mathematics page: Knotoids. <http://www.layer8.co.uk/maths/knotoids/index.htm>, 2015.

- [2] J. S. Carter, D. Jelsovsky, S. Kamada, L. Langford, and M. Saito. Quandle cohomology and state-sum invariants of knotted curves and surfaces. *Trans. Amer. Math. Soc.*, 355(10):3947–3989, 2003.
- [3] J. Cenicerós, M. Elhamdadi, M. Green, and S. Nelson. Augmented biracks and their homology. *Internat. J. Math.*, 25(9):1450087, 19, 2014.
- [4] M. Elhamdadi and S. Nelson. *Quandles—an introduction to the algebra of knots*, volume 74 of *Student Mathematical Library*. American Mathematical Society, Providence, RI, 2015.
- [5] R. Fenn, C. Rourke, and B. Sanderson. Trunks and classifying spaces. *Appl. Categ. Structures*, 3(4):321–356, 1995.
- [6] D. Goundaroulis, J. Dorier, F. Benedetti, and A. Stasiak. Studies of global and local entanglements of individual protein chains using the concept of knotoids. *Scientific Reports*, 7, 2017.
- [7] D. Goundaroulis, N. Gügümcü, S. Lambropoulou, J. Dorier, A. Stasiak, and L. Kauffman. Topological models for open knotted protein chains using the concepts of knotoids and bonded knotoids. *Polymers, Special issue on Knotted and Catenated Polymers*, 9, 2017.
- [8] N. Gügümcü. On knotoids, braidoids and their applications. *PhD thesis, NTUA*, 2017.
- [9] N. Gügümcü and L. H. Kauffman. New invariants of knotoids. *European J. Combin.*, 65:186–229, 2017.
- [10] N. Gügümcü and L. H. Kauffman. On the height of knotoids. In *Algebraic modeling of topological and computational structures and applications*, volume 219 of *Springer Proc. Math. Stat.*, pages 259–281. Springer, Cham, 2017.
- [11] N. Gügümcü and S. Lambropoulou. Braidoids. *submitted*.
- [12] N. Gügümcü and S. Lambropoulou. Knotoids, braidoids and applications. *Symmetry, Special Issue: Knot Theory and Its Applications*, 9(12), 2017.
- [13] L. H. Kauffman. Virtual knot theory. *European J. Combin.*, 20(7):663–690, 1999.
- [14] S. Nelson, M. E. Orrison, and V. Rivera. Quantum enhancements and biquandle brackets. *J. Knot Theory Ramifications*, 26(5):1750034, 24, 2017.
- [15] S. Nelson and N. Oyamaguchi. Trace diagrams and biquandle brackets. *Int. J. Math.*, 28(14):24, 2017.
- [16] M. Niebrzydowski. Biquandle longitude invariant of long virtual knots. *J. Knot Theory Ramifications*, 16(10):1393–1401, 2007.
- [17] V. Turaev. Knotoids. *Osaka J. Math.*, 49(1):195–223, 2012.

DEPARTMENT OF MATHEMATICS
 NATIONAL TECHNICAL UNIVERSITY OF ATHENS
 ZOGRAPHOU CAMPUS, IROON POLYTECHNIQ 9
 ATHENS 15780, GREECE

DEPARTMENT OF MATHEMATICAL SCIENCES
 CLAREMONT MCKENNA COLLEGE
 850 COLUMBIA AVE.
 CLAREMONT, CA 91711